Materiales de Construcción
Vol. 67, Issue 328, October–December 2017, e141
ISSN-L: 0465-2746
http://dx.doi.org/10.3989/mc.2017.10116

Accelerated action of external sulfate and chloride to study corrosion of tensile steel in reinforced concrete

M. A. G. Silva[a]✉, M. P. Cunha[b], A. Pinho-Ramos[a], B. Sena da Fonseca[c], F. F. S. Pinho[d]

a. Faculdade de Ciências e Tecnologia, Universidade Nova de Lisboa, (Caparica, Portugal)
b. Instituto Universitário da Maia, (Maia, Portugal)
c. Centro de Química Estrutural-CQE, Instituto Superior Técnico, Universidade de Lisboa, (Lisboa, Portugal)
d. CERIS, Faculdade de Ciências e Tecnologia, Universidade Nova de Lisboa, (Caparica, Portugal)
✉ mgs@fct.unl.pt

Received 30 August 2016
Accepted 1 March 2017
Available on line 5 October 2017

ABSTRACT: Corrosion of the reinforcing steel may cause significant loss of strength of reinforced concrete structures. The study focuses on accelerating such corrosion and examining the degradation of (i) the compressive strength of concrete due to sodium sulfate in a wet atmosphere; and (ii) the flexural strength by a solution of sodium sulfate and sodium chloride. Three types of concrete were used and different beam specimens were reinforced by steel rebars of different diameters (6, 8 and 10mm), part of the beams being pre-cracked. The concrete with least strength allowed higher sulfate penetration along the entire process and the compressive strength increased slightly, possibly due to lower porosity of concrete after contamination. The results of the flexural tests showed decrease of strength in all cases. Pre-cracked beams exhibited smaller influence of porosity of concrete. Beams with 6mm rebars showed the largest loss of strength due to the contamination and corrosion process.

KEYWORDS: Steel; Concrete; Sulphate attack; Durability; Corrosion.

Citation/Citar como: Silva, M.A.G.; Cunha, M.P.; Pinho-Ramos, A.; Sena da Fonseca, B.; Pinho, F.F.S. (2017) Accelerated action of external sulfate and chloride to study corrosion of tensile steel in reinforced concrete. *Mater. Construcc.* 67 [328], e141 http://dx.doi.org/10.3989/mc.2017.10116

RESUMEN: *Acción externa acelerada de sulfatos y cloruros en el estudio de la corrosión del acero en tracción en el hormigón armado*. La corrosión de la armadura de acero de refuerzo puede causar una disminución de la resistencia de las estructuras de hormigón armado. Este estudio se centra en la aceleración artificial de tal corrosión examinando la degradación (i) de la resistencia a compresión del hormigón debida al sulfato de sodio en medio húmedo; y (ii) de la resistencia a flexión causada por una solución de sulfato de sodio y cloruro de sodio. Se han utilizado tres clases de hormigón y vigas con refuerzo de diferentes diámetros (6, 8, 10 mm); algunas de las vigas fueron pre-fisuradas. El hormigón con menor resistencia permitió mayor penetración de los sulfatos y la resistencia a compresión aumentó, posiblemente debido a la menor porosidad después de la contaminación. Los ensayos de flexión mostraron que la resistencia decrecía en todos los casos. Las vigas pre-fisuradas mostraron menor influencia de la porosidad. Las vigas armadas con barras de 6 mm de diámetro tuvieron mayor pérdida de resistencia.

PALABRAS CLAVE: Acero; Hormigón; Ataque por sulfatos; Durabilidad; Corrosión

ORCID ID: M. A. G. Silva (http://orcid.org/0000-0002-0379-9642); M. P. Cunha (http://orcid.org/0000-0002-5889-5543); A. Pinho-Ramos (http://orcid.org/0000-0001-9496-4991); B. Sena da Fonseca (https://orcid.org/0000-0003-2166-0430); F. F. S. Pinho (http://orcid.org/0000-0003-0344-1867)

1. INTRODUCTION

The main objective of this paper is the study of the feasibility of accelerating the corrosion of steel reinforcement due to contamination by sulfates.

The results generated by techniques that accelerate aging processes face the problem of their generalization to actual conditions, a question not addressed here due to its complexity. Such generalization requires simultaneous consideration of the several variables that can be differently accelerated and available techniques that e.g. use Arrhenius-like procedures (1) would require a specific separate treatment.

Some of the accompanying consequences of the accelerated process of steel corrosion on the whole of the reinforced concrete (RC) structures are also reported. The attack of RC structures by external sulfates is known, but scarcely studied. Sulfate ions or sulfur dioxide are harmful to RC structures and contribute to the reduction of their life-cycle (2, 3) and cases of sulfate attack of above ground structures in the United Kingdom and in the United States, including in some highway structures have been reported e.g. by Vittery and Pearson-Kirk in (4).

Sewage systems often present signs of superficial deterioration of concrete with dissolution of cement paste and the main deterioration located above the water level (5) in a process that involves sulfates. Figure 1 shows evident deterioration of concrete in a waste water treatment plant in Portugal a few years after its opening, a problem equally present in Canada (6) where degradation of the exterior walls was attributed to sulfur-rich water and soils. Another source of aggression by sulfates is the combustion of coals (especially lignites) and heavy fuel-oils that produces flue gases containing large amounts of sulfur dioxide (7, 8) that degrade the power plant stacks.

The mechanism most used for explaining the degradation of the concrete when subjected to media rich in sulfate ions was proposed by Atkinson and Herne (3) and validated at the National Institute of Standards and Technology (NIST) (9). The method requires the determination of the diffusion coefficient of sulfate ions into concrete (2). De-icing salts are also a common cause of degradation by sodium chlorides and potassium acetate present in sulfate contaminated soils. Concrete under chemical attack of aqueous solutions of sulfates suffers changes in the microstructure and modifies the distribution of the pore sizes. The chemical reactions create products of larger volume than the original materials. Such expansions originate cracks, increase the permeability of concrete and cause loss of strength and mass with time.

The two main mechanisms of sulfate attack are: (i) reaction with monosulfate hydrate, calcium aluminate hydrate, and/or unhydrated tricalcium aluminate to produce ettringite; and (ii) reaction with calcium hydroxide ($Ca(OH)_2$) to produce calcium sulfate (gypsum – $CaSO_4$) (10).

Similar phenomena to the above occur when RC is submitted to moist environments containing dioxide sulfur. The dioxide sulfur (SO_2) reacts with water (H_2O) and forms sulfuric acid (H_2SO_4) that ultimately reacts with several concrete compounds. Despite the multiplicity of the process and the formation of several compounds, the primary product of alkaline compounds decomposition by sulfuric acid is calcium sulfate (pH≈7.7) (11, 12). Ideal conditions for the corrosion onset of steel reinforcements are then established when the concrete cover becomes more permeable and less alkaline.

Chloride ions depassivate steel and corrosion rate becomes rather significant (13) when a threshold of the concentration is reached at the depth of steel bars. At low pH values, as for concrete damaged by sulfates or sulfuric acid, the corrosion initiation can take place at significant lower concentrations of oxygen and chlorides (14).

In a real environment the combined effect of sulfate and chloride has been found to be yet more damaging for the structural integrity of reinforced concrete and this conclusion bears the decision taken in the present study to switch, at a given time, from sulfates only contamination to a combination of sulfates and sodium chloride (15–18).

Noticing that there is no standard for the study of concrete contamination by sulfur dioxide, the

FIGURE 1. Aspects of concrete degradation. Waste treatment unit. Aveiro, Portugal.

work described hereafter followed partially ASTM G 87–02 meant to evaluate the resistance of organic coatings (19).

Standards available to evaluate concrete behavior when exposed to sulfate ions include ASTM C 452 (20) and ASTM C 1012 (21) but the former is not applicable to Portland cement. ASTM C 1012 defines the submission of concrete specimens to a solution of sodium sulfate, 50 g/l, for six months to measure the expansion of the specimens.

This brief review established that, in addition to damage caused by the late release of sulfate ions originating from contaminated sources of aggregates, external sulfate attack (ESA) is a source of concern and corrosion of steel (22) and the primary object of the present study is to simulate experimentally such corrosion within a short time frame by electrochemical acceleration of the process.

2. MATERIALS AND METHODS

2.1. Chamber Contamination

For the assessment of contamination by SO_2, four beams 600x150x100 (mm) of reinforced concrete C1 (see Table 1) were built using cement type CEM II/A-L 32.5R (23), and four 8 mm steel rebars, with a 20 mm concrete cover. Cubes of the same concrete mix with side of 150mm were also made. The beams and four cubes were placed in a SO_2 contamination chamber Damp Heat Chamber and subjected to an environment with 3.3% of SO_2 in total volume of air (a 10 times percentage higher than the recorded average in this zone) at a temperature of 40 °C, without ventilation, for two consecutive terms of 1000 hours (h) each. The strength characterization was made by compression tests and taken as reference at the beginning of the contamination. The compressive strength was also evaluated after 1000h and 2000h of contamination.

At each of those stages of contamination, two beams were removed from the chamber and subjected to flexural strength tests. Samples of concrete powder were collected at depths of 20mm and 40mm, taken from small diameter drilled holes. The determination of sulfates percentage in the concrete, by weight, was made according to (24, 25) and the initial concentration of free sulfates in the beams was considered negligible.

2.2. Contamination by sulfates and chloride solution

2.2.1. Specimens to be contaminated

Two sets of 15 beams, manufactured with a geometry defined by a square cross section with sides of 150mm and a length of 600mm, were subjected to accelerated contamination by sulfate and chloride ions. Each set corresponded to a different mix as characterized in Table 1 (concretes designated as C2 and C3), but both batches were made using the same cement type, as before. The introduction of 35% more fly ashes and 37.5% more cement, per cubic meter, in the mix of C3 versus that of C2, led to the reverse decrease of 20% of sand as customary in the industry of construction, leading to a concrete C3 with higher strength and lower porosity (7.7% vs. 10.6% as detailed below) than those found for C2.

Each beam was reinforced with 2 longitudinal rebars. The diameters differed from beam to beam as shown in Table 2 that refers only to the contaminated beams, 6 more having been built for control, two per each bar diameter. To further study the influence of cracking in the contamination process, some of the beams were pre-cracked before the beginning of the contamination protocol. This was achieved loading those beams with a concentrated force at mid-span that generated the cracking bending moment. For each concrete, and for each rebar size, five beams were cast (one reference beam not to be contaminated, two non-cracked and two pre-cracked to be subjected to contamination). The concrete cover clearance of the longitudinal reinforcement was 20mm.

Concrete cubes (150mm side) were also cast along with the beams and were used to assess the concrete strength. The results for the concrete compressive strength (f_{ccm}) at 28 days were 46.8MPa for C2, and 50.7 MPa for C3. The values for C2 and C3 were tested again after 850 days and the compressive strength found was higher, averaging, respectively, 64.3MPa and 70.5MPa.

Table 2. Characteristics of the beams

Concrete type	Non cracked	Pre cracked
C2	2 ϕ6, 2 ϕ8, 2 ϕ10	2 ϕ6, 2 ϕ8, 2 ϕ10
C3	2 ϕ6, 2 ϕ8, 2 ϕ10	2 ϕ6, 2 ϕ8, 2 ϕ10

Table 1. Composition of concretes C1, C2 and C3

Concrete	Cement (kg/m^3)	Sand (kg/m^3)	Gravel (4-12.5) (kg/m^3)	Gravel (12.5-25) (kg/m^3)	Fly ash (kg/m^3)	Pozzolith 5.4 (kg/m^3)	Water (l/m^3)
C1	280	810	500	550	-	3	160
C2	200	800	510	560	100	3	175
C3	275	640	550	580	135	4.1	165

The tensile strength properties of the reinforcement steel bars ϕ6, ϕ8 and ϕ10 were obtained from tensile tests and the values found for the yield strength (f_y) were, respectively, 523 MPa, 550 MPa and 542 MPa. For the ultimate strength (f_t), in the same order, 618 MPa, 697 MPa and 669 MPa.

2.2.2. Contamination Protocol

The contamination by sulfate and chloride ions was started after concrete was cured for 28 days at 20 °C and 90% RH (23). A small acrylic container was installed having the bottom on the tensile side of the beam, as shown in Figure 2. Inside the container a thin sponge was positioned under a stainless steel mesh, and connected to a copper conductor. After assemblage, the container was partially filled with a solution of sodium sulfate and sodium chloride at 5% and 3% by weight, respectively.

At mid-height and mid-length of each of the beams to be contaminated, a grid of A304 stainless steel was placed, connected to a copper wire linked to an external circuit, as sketched also in Figure 2. Both conductors were connected to a DC voltage source (Sorensen, XHR 40–25). A current density between 2 and 4mA/cm^2 was applied between the stainless steel meshes to generate a constant electric field that accelerated contamination of the concrete by the ions contained in the solution. The contamination process was conducted during a 9 week period on the beams cast with the concrete mix of smaller strength (C2) and 12 weeks for the beams made with the stronger concrete (C3). The reason for the different times adopted was the difference of porosity between C2 and C3. Every 3 or 4 weeks, concrete powder samples were obtained by drilling 10mm to 20mm deep into the beams, the distances bring measured from the top surfaces. The determination of the sulfates percentage in the concrete powder followed (24, 25).

The level of alteration on the concrete microstructure and any eventual formation of major mineralogical phases were studied via X-ray diffraction analysis and mercury intrusion porosimetry performed both in plain and contaminated concrete.

3. RESULTS AND DISCUSSION

For easier reference and interpretation, the results associated with SO_2 contamination in wet atmosphere, in a climatic chamber, are reported separately from those corresponding to the attack on a restricted area of the outer surface of beams by a solution of chloride and sulfate.

3.1. SO_2 contamination in climatic chamber

3.1.1. Effects on concrete compressive strength

The amounts of sulfate present in the samples obtained at depths of 20mm and 40mm, after 1000h of contamination in the SO_2 chamber, were respectively 0.58% and 0.40%. At 2000h the values changed to 1.20% and 0.64%. The SO_2 beams contamination is expressed by: $\frac{ion\,sulfate\,mass}{concrete\,mass}$ percentage.

Despite the 2000 h of contamination, the percentage of sulfates found in the concrete is very small. This small contamination values achieved in the cubes, only 1.2% (maximum value), shows how the natural process of contamination can be slow for a concrete of good composition.

The 28 days average compressive strength of the reference concrete cubes, i.e. those without contamination (C1), was 29.3MPa. The cubes subjected to 1000h of SO_2 contamination showed a mean strength of 32.0MPa, whereas at 2000h the value was 31.0MPa, i.e. it remained approximately constant. The failure of the reference samples, unlike the case of the contaminated samples, was accompanied by the projection of numerous debris, evidencing that the contaminated samples became less brittle. It is suggested that crystals, resulting from the reaction between the cementitious materials and SO_2, partially filled concrete pores, and their continued formation and growth induced internal stresses and cracking. Expectable decrease of strength ensued as the contamination proceeded. The surfaces of contaminated cubes also showed a yellowish color due to chemical alteration as previously described in the literature (27).

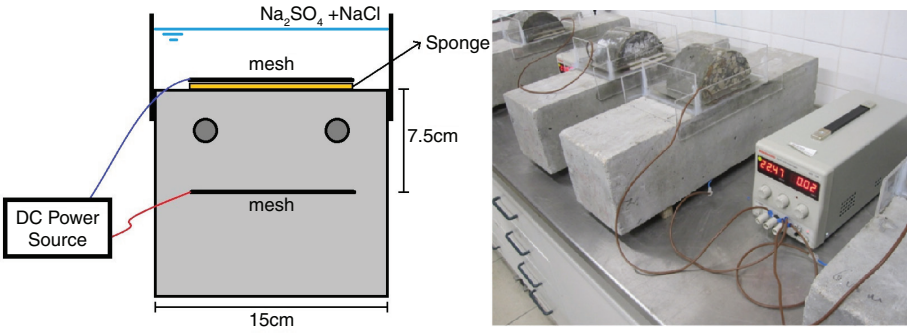

FIGURE 2. View of the external container with stainless grid. A weight is placed over the grid to maintain pressure on sponge.

3.1.2. Effects of SO_2 in concrete flexural strength

The contamination in the SO_2 chamber proved to be insufficient to cause significant effects in the flexural behavior. This was perhaps because the sulfate contamination occurred only on the surface as a result of the short time of actual aging due to technical limitations of the chamber which did not allow sustained application of higher rates of contamination. In addition, these initial concrete specimens were conceived essentially to verify the effectiveness of the process to accelerate the corrosion of the steel and the diameter of the reinforcement bars versus the geometry of the beams was not representative of what would be required for them as structural members, i.e. the reinforcement was excessive. Despite that, flexural tests were performed after contamination and the results obtained in two beams subjected to 1000h and 2000h of contamination, respectively, were compared. The values obtained indicated higher failure load after 2000h (39 versus 32 kN), a fact difficult to interpret since the compressive strength of concrete, as previously seen, was not altered.

3.2. Sulfate and chloride ions contamination

The contamination of the beams increased over time and could be observed on the lateral faces of the beams. Figure 3 shows, as a representative case, the central part of a lateral face of one beam reinforced with 10mm rebars and cast with concrete C3. The parameters chosen to characterize the effects of the penetration of sulfate ions into the beams are examined below.

3.2.1. Concrete resistance

The electric resistance of the wires, connections and steel mesh was considered negligible when compared to the electric resistance of the concrete electrolyte and the electric resistance of some specimens produced by possible electrode reactions in the presence of oxygen. This electric resistance was calculated according to the first law of Ohm, R=U/I, where U is the electric potential and I is the current intensity in the circuit. Figure 4 illustrates representative cases of the electrical resistance evolution during the time of contamination of the beams.

The total porosities calculated by Hg intrusion and the corresponding pores size distribution are shown in Figure 5. As expected, concrete C2 is considerably more porous than C3. This difference was reflected in the overall concrete electrical resistance and had implications on the beams contamination through differential ionic current flows. Despite the different porosities, the pore size distribution in each mortar is quite similar.

Along the process of contamination the beams cast with C3 concrete showed consistently higher electrical resistance values than those of the beams cast with C2, despite the influence on the ion transport process of the electric field applied, i.e. the initial concrete porosity controled the ionic current flow, see Figure 4.

In general, as the contamination process advanced the electrical resistance of the system tended to increase. This might be due to the production of substances from the electrodes reaction

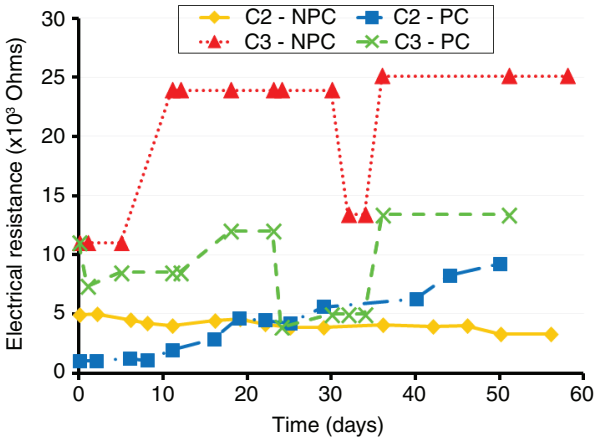

FIGURE 4. Representative electrical resistance evolution during beams contamination (6mm).

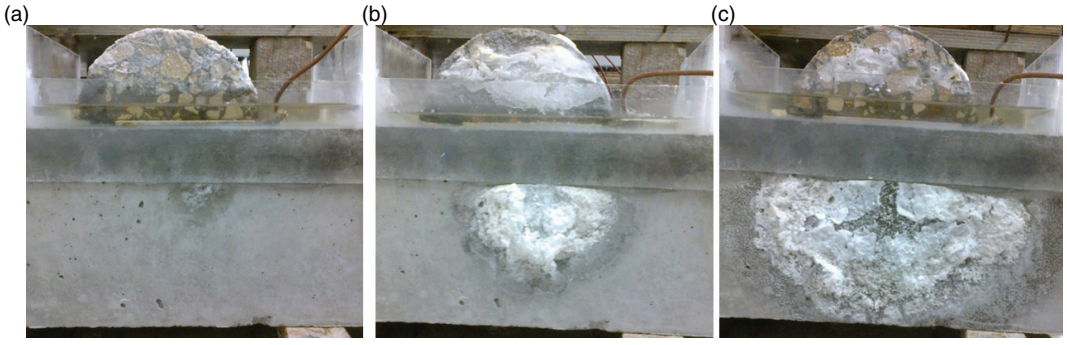

FIGURE 3. Salts deposited on the lateral surface of the beam after 3 days (a), 40 days (b) and 84 days (c) of contamination. Concrete C3 and 10 mm rebars.

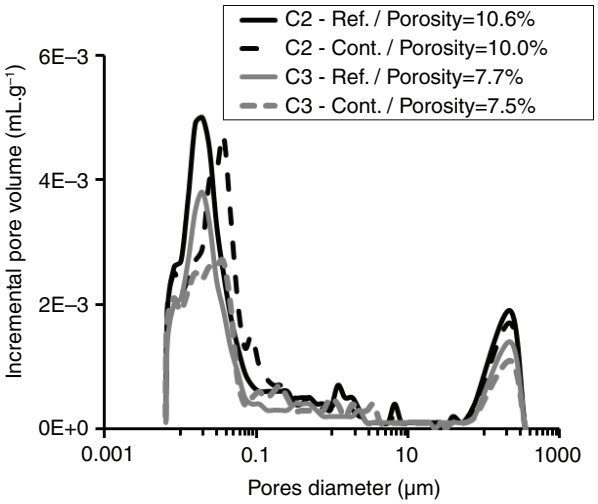

FIGURE 5. Pore size distributions of concrete mortar before (ref.) and after contamination.

in the presence of oxygen, and to the reaction of sulfate ions with the tricalcium aluminate ($3CaO.Al_2O_3$) present in the cement. Reaction of the sulfate ions with tri-calcium aluminate, first, formed calcium sulfo-aluminates and then ettringite, and the resulting new crystals partially filled the pores, further reducing the solution uptake and explaining the increase of the electrical resistivity in the beams, as previously found by Cunha (26).

The larger electric resistance of concrete caused by the decrease of porosity, also decreased the diffusion or mass transport process. However, the speed of the corrosive process was no longer controlled by diffusion but by the presence of free chloride ions near the rebar. This change in the corrosive mechanism can explain the corrosion detected in the rebar.

After a few weeks of contamination, the beams showed oxides leaching at mid-level of the lateral faces. The accumulation of corrosion products, salt crystallization and weakness due to the introduction of the mesh created parallel cracks in the zone of the mesh. The mesh and ensuing parallel cracks, though located at the region of lowest stresses, required careful attention when changes of mechanical strength were analyzed.

Concrete-mesh adhesion was deteriorated by the presence of corrosion products between the mesh and the steel bars. This loss of adhesion between the mesh and the concrete did not occur in non-pre-cracked beams.

3.2.2. Concrete contamination and sulfate/chloride penetration

The chemical and microstructural damage of concrete due to multiple deterioration mechanisms associated with the combined action of sulfate and chloride involves numerous chemical phenomena and resultant products. Such complexity required thorough analyses and, despite not being a central target of this research, an effort was placed to identify major chemical/microstructural changes caused by the contamination protocol. In order to measure the changes on the microstructure, small pieces of the cement matrix were obtained both from the reference and contaminated concrete beams (non-cracked). Both concrete mortars evidenced a negligible change in porosity due to the contamination, especially C3. However, through the pore size distributions, it was possible to detect important differences in the microstructures after the contamination. Generically, the volume of pores with diameters below 0.025μm (25nm) decreased, whereas, the volume of pores with diameters ranging between 0.025μm and 0.200μm increased. The likely cause is that crystallized salts and/or reaction products between the contaminants and the cement components remained in the system. Another reason is the appearance of micro-cracks due to salts crystallization. Both contributed to significant modifications on the concrete microstructure that affected the transport phenomena.

To investigate the eventual development of new mineral forms during the contamination, the cement paste was also analysed by x-ray diffraction, Figure 6. In all cases, for both concrete types and in pre-cracked and non-cracked beams, gypsum and halite were identified. The major peaks identified in all samples corresponded to quartz and calcite whose presence is attributed to the concrete aggregates (limestone and siliceous sand). In all the contaminated specimens, additional peaks appeared that were attributed to gypsum and halite. These new mineral forms are a consequence of concrete contamination by sulfates and chlorides, respectively. While the occurrence of halite did not indicate any reaction between the cement components, the presence of gypsum confirmed chemical reactions between sulfates and cement alkaline compounds. It was not possible to identify ettringite and thaumasite, probably because the contamination did not last long enough to allow the generation of significant quantities.

Several studies (28, 29) have indicated that chloride ions diffuse much faster than sulfate ions into hardened cement paste. Oberholster reported that the diffusion of chloride ions in concrete is generally 10 to 100 times faster than that of sulfate ions (28). It was thought reasonable to accept that the same happened when applying a constant electric field to *push* these ions into the concrete.

The presence of sulfate ions in the chloride solution did not influence the initiation time of the chloride-induced reinforcement corrosion, but the rate of corrosion increased with increasing sulfate concentration. That occurred because the tricalcium aluminate in the concrete also binds to sulfate ions,

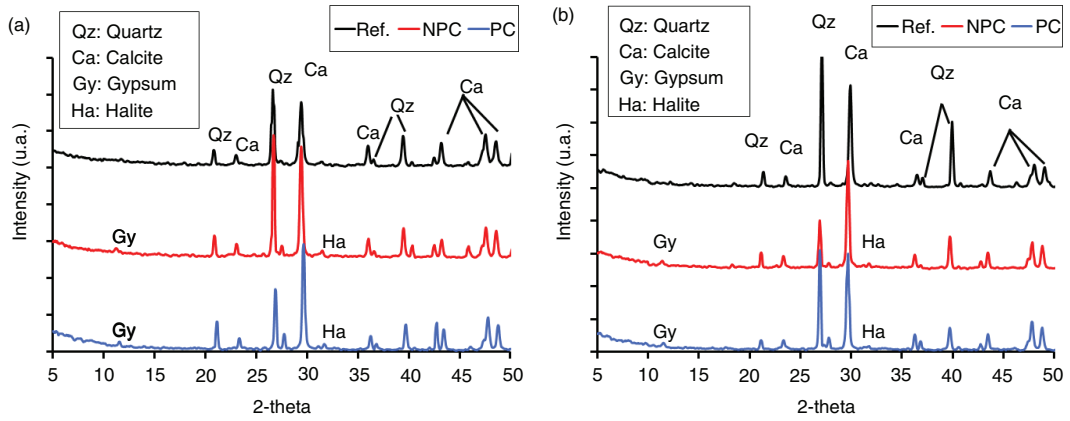

FIGURE 6. X-ray diffraction patterns of concrete mortar C2 (a) and C3 (b), before (ref.) and after contamination.

and because the amount of free chloride also intensified the corrosive process.

Accordingly the fast corroding process verified in the rebars is attributed to the high concentration of free chloride ions carried by the applied electric field, and not to the presence of sulfate ions.

Figure 7 displays the evolution in time of the quantity of sulfates in the concrete. The data represent the mean values of the gain of mass of sulfates found for each type of beam.

At the end of the contamination process of the specimens C2 and C3, for 9 and 12 weeks, respectively, the results obtained varied between 0.04g and 0.06g sulfate per 5g of concrete. That matches the percentages of sulfate contamination between 0.8% and 1.2% found in the concrete mass.

Dispersion of the observed results was expected due to the heterogeneity of concrete, reflected in the contents of powder samples taken at different horizontal plane locations and depths. Nonetheless, some conclusions can be advanced from the mean values found.

- The quantity of sulfates found in the specimens varied with the concrete mix. Concrete C2, the one with smaller strength, allowed higher sulfate penetration all along since the beginning of contamination.
- In non-pre-cracked beams the porosity had a more important role in the diffusion of the sulfates.
- In pre-cracked beams the relative importance of the type of concrete and its porosity were lower both in terms of penetration and total uptake of the solution.

3.3. Results from Bending Tests

Essentially, two types of tests were carried out to examine the effects of the described contamination on the concrete beams:

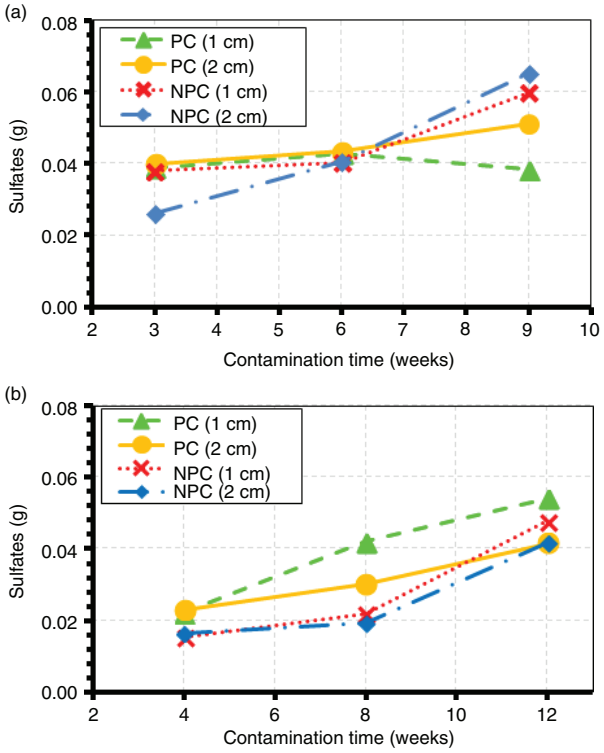

FIGURE 7. Sulfate amount for as-built and pre-cracked concrete beams along contamination, concrete C2 (a) and concrete C3 (b).

- Three point bending tests of the specimens reinforced with 6 mm and 8 mm rebars and the concentrated load applied at mid-span on the face opposite to the contaminated face;
- Tensile strength of the 10mm reinforcing steel bars removed from the corresponding beams after after having submitted these beams to the same type of loading as those reinforced with 6mm and 8mm rebars. The option for the tensile tests was due to the fact that hypercritical reinforcement and short span of those beams did

not allow comparative analysis of the results by engineering beam theory.

Figure 8 summarizes the data obtained from the flexural tests in the beams reinforced with 6 mm rebars, where "Ref" designates the reference beam without contamination, and PC and NPC refer to the pre-cracked and non-pre-cracked specimens, respectively. The results evidenced the detrimental effects of corrosion caused by the contamination, showing a decrease of the maximum strength of approximately 27% for concrete C2 and 22% for concrete C3, due to the contamination. It is noticed that the mix for concrete C3 had, compared with C2, more cement, more fly ashes and more pozzolith 540 and less water that led to lower porosity and explain the smaller influence of contamination.

The differences observed between the strength of specimens PC and NPC were small, though for concrete C3, the pre-cracked beams showed a slightly lower strength than the non-pre-cracked beams. This is attributed to the additional penetration of sulfate caused by the pre-cracks.

Signs of corrosion products around the rebars and salt crusts were seen after the flexural tests on the beam surface opposite to the face directly contaminated in one of the pre-cracked beams with 6 mm rebars.

Figure 9 shows the results from the bending tests performed on the beams with 8 mm rebars. For concrete type C2 the beams subjected to contamination showed a decrease of maximum strength of about 9% and 5%, for the PC and NPC specimens, respectively. A similar behavior was observed in the beams made of concrete C3, but with a more accentuated decrease of strength, 18% and 13%, when compared to the values found for the reference beam.

The corrosion of the rebars occured more heterogeneously in the pre-cracked beams. Corrosion was also detected where the cracks intersected the rebars. In the NPC beams corrosion was more homogeneous along the rebars due to the absence of the pre-cracks as preferential paths. On average, the decrease of strength was smaller than that observed in the beams with 6mm rebars, since the 6mm rebars

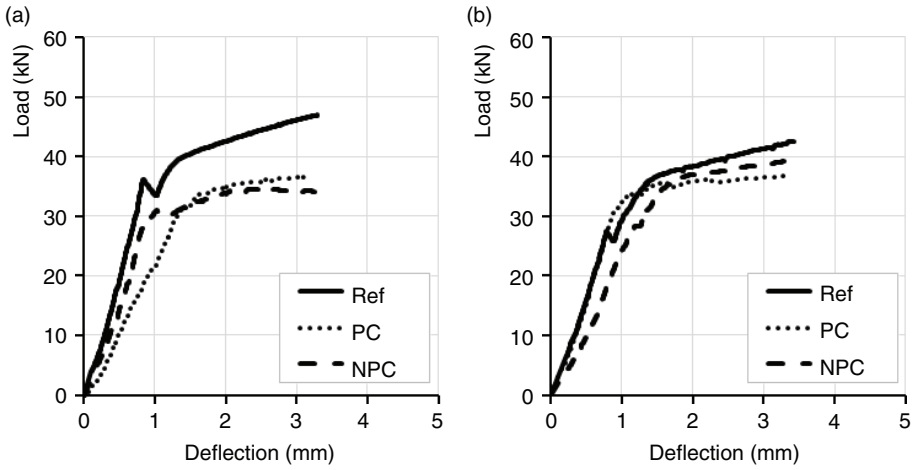

FIGURE 8. Experimental results from the flexural tests for the 6mm rebars beams, concrete C2 (a) and concrete C3 (b).

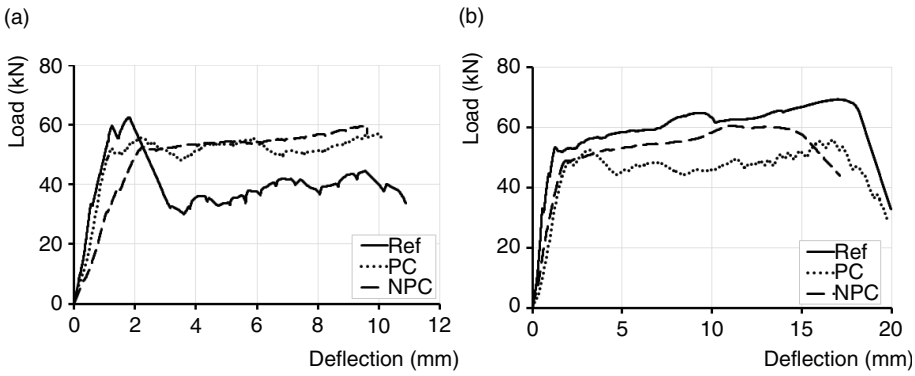

FIGURE 9. Experimental results from the flexural tests for the 8mm rebars beams, concrete C2 (a) and concrete C3 (b).

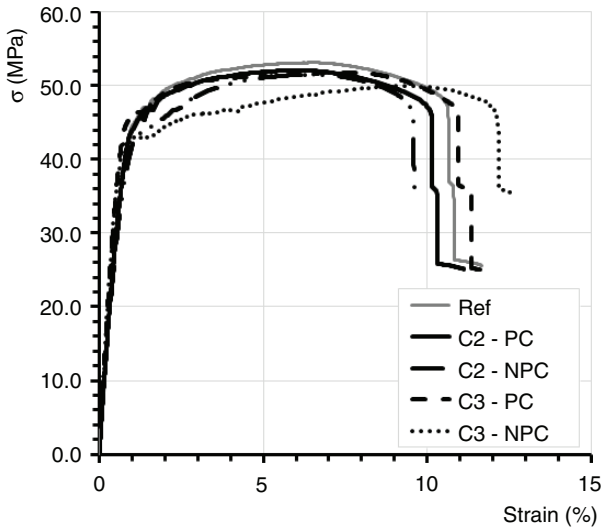

FIGURE 10. Experimental results from the tensile tests of 10 mm rebars (C2 and C3).

had a higher specific surface, and were thus more susceptible to corrosion.

Figure 10 presents the results obtained from the tensile tests performed on the rebars extracted from the contaminated beams, after carefully removing the surrounding concrete. To be used as reference values, three coupons from the steel samples had not been subjected to the contamination processes and the average results for their tests are also shown in Figure 10 and identified as "Ref". The decrease of strength between the reference and the contaminated specimens was small, varying between 2% and 6%.

It can be observed that the contamination protocol was also efficient for the 10mm rebars, but in order to get more visible results the contamination process should be longer.

4. CONCLUSIONS

Briefly, it can be stated that

- An accelerated contamination of reinforced concrete elements with sulfates was successfully applied. The study showed the feasibility of using an electrochemical procedure, associated with a protocol that implemented direct contact of the contaminant solution on the beams, as an effective way to accelerate the corrosion of the steel reinforcement.
  Ways of establishing temporal correspondence of these tests with real cases remain a challenge for future work.
- The use of a contamination chamber of SO_2 creating an atmosphere with 3.3% volume of SO_2 and high humidity presented experimental limitations hard to overcome.
- In terms of experimental results:
  i) The contamination in the climatic chamber showed small upwards change of concrete compressive strength, after 1000h and 2000h of exposure.
  ii) Under the direct contact of the contaminant solution with the surface of the beams,
    - The ingress of sulfates and chlorides led to depassivation of rebars and severe corrosion.
    - Cracking played important part in the corrosion process.
    - In non-pre-cracked beams the class of concrete had a larger role in aggressive ions uptake and damage, with more penetration of sulfates for the concrete with lower compressive strength, as expected;
    - The importance of the porosity of concrete on the total penetration of the sulfate solution was superseded by the importance of the pre-cracks. In non-pre-cracked beams the porosity of concrete was a more important parameter;
    - In the beams reinforced with 6mm rebars the largest decrease of strength was observed, due to the contamination and ensuing corrosion process. This observation can be explained by the fact that the 6mm rebars have a higher specific surface, thus being more susceptible to corrosion.

On average the decrease of strength varied between 22% to 27% for the specimens reinforced with 6 mm rebars, 5% to 18% for the 8mm, and 2% to 6% for the 10mm.

Although the electrochemical procedure, associated with the direct contact of the contaminant solution with the beams, proved to be a viable and effective means to accelerate corrosion of reinforced concrete structures, studies that include a longer period of the contamination are needed, in order to cause higher levels of corrosion, especially for larger diameter bars and bigger concrete cover.

ACKNOWLEDGMENTS

The authors are grateful to Fundação para a Ciência e Tecnologia for partial financing of the work under Project PTDC/ECM/100538/2008.

REFERENCES

1. Silva, Manuel A G., Sena da Fonseca, B., Biscaia, Hugo. (2014) On estimates of durability of FRP based on accelerated tests, Composite Structures 116 377–387. https://doi.org/10.1016/j.compstruct.2014.05.022
2. Metha, P. K. (1992) Sulfate Attack on Concrete – a Critical Review. Materials Science of Cement III. J. Skalny (Ed.) ACS
3. Atkinson, A. and Herne, J. A. (1990) Mechanistic Model for the Durability of Concrete Barriers Exposed to Sulfate Bearing Groundwaters", Materials Research Society Symposium Proceedings, 176, 149–156. https://doi.org/10.1557/PROC-176-149

4. Vittery, J. P., Pearson-Kirk, D., (2008). Sulfate Induced Deterioration of Above Ground Components of Highway Structures, Structural Faults + Repair, 12th International Conference.
5. Fernandes, I., Pericão, M., Hagelia, P., Noronha, F., Ribeiro, M. A., and J. Maia (2009). Identification of Acid Attack on Concrete of a Sewage System. 12th Euroseminar on Microscopy Applied to Building Materials, Dortmund, Germany.
6. Iggy, I.P., B.A.Sc., E.I.T. (2005) "Sulfur attack on concrete tanks – A problem in the on-site wastewater industry that needs to be addressed". Ontario Onsite Wastewater Association Newsletter 6.
7. Demirbaş, A., T. Öztürk, Faik Özgür Karataş (2001) Long-term wear on outside walls of buildings by sulfur dioxide corrosion. *Cem. Concr. Res.* 31(1): 3–6. DOI: 10.1016/S0008-8846(00)00447-6
8. ApSimon, H. M. and D. Cowell (1996) The benefits of reduced damage to buildings from abatement of sulfur dioxide emissions. Energy Policy 24(7): 651–654. https://doi.org/10.1016/0301-4215(96)00058-4
9. Pommersheim, J. M. Clifton J. R. (1994) Expansion of Cementitous Materials Exposed to Sulfate Solutions. Materials Research Symposium Proceedings 333, 363–368.
10. Monteiro P., Roesler J., Kurtis K., Harvey J. (2000) - Accelerated Test for Measuring Sulfate Resistance of Hydraulic Cements for Caltrans LLPRS Program. Report. Pavement Research Center, Institute of Transportation Studies, University of California, Berkeley. p.46.
11. Marinoni, N., M. P. Birelli, C. Rostagno, A. Pavese (2003). The effects of atmospheric multi-pollutants on modern concrete. Atmospheric Environment 37(33): 4701–4712. https://doi.org/10.1016/j.atmosenv.2003.06.001
12. Okun D.A, Wang L.K., Shammas N.K. (2010) Water Supply and Distribution and Wastewater Collection. John Wiley and Sons.
13. Boubitsas D., Tang L. (2015) The influence of reinforcement steel surface condition on initiation of chloride induced corrosion. *Mat. Struct.* 48(8): 2641–2658. https://doi.org/10.1617/s11527-014-0343-2
14. Berke, N. S., Chaker, V. (1990). Corrosion rates of steel in concrete (No. 1065). ASTM International. https://doi.org/10.1520/stp1065-eb
15. Dehwah, H. A. F., M. Maslehuddin, S.D. Austin (2002). Long-term effect of sulfate ions and associated cation type on chloride-induced reinforcement corrosion in Portland cement concretes. *Cem. Concr. Comp*. 24(1): 17–25. https://doi.org/10.1016/S0958-9465(01)00023-3
16. Zuquan, J., S. Wei, Z. Yunsheng, J. Jinyang, L. Jianzhong (2007). Interaction between sulfate and chloride solution attack of concretes with and without fly ash. *Cem. Concr. Res.* 37(8): 1223–1232. https://doi.org/10.1016/j.cemconres.2007.02.016
17. Hobbs, D. W. and M. G. Taylor (2000). Nature of the thaumasite sulfate attack mechanism in field concrete. *Cem. Concr. Res.* 30(4): 529–533. https://doi.org/10.1016/S0008-8846(99)00255-0
18. Ba, M., C. Qian (2012). Effects and mechanism of atmospheric multi-acidic gases on cement-based concrete linings of vehicle tunnels. *Constr. Build. Mat.* 29(0): 438–443. https://doi.org/10.1016/j.conbuildmat.2011.09.016
19. ASTM G 87–02 Standard (2007). Practice for Conducting Moist SO_2 Tests. West Conshohocken, PA
20. ASTM C 452 Standard (2010). Test Method for Potential Expansion of Portland Cement Mortars Exposed to Sulfate (ASTM Philadelphia, P.A.).
21. ASTM C 1012 Standard (2012). Test Method for Length Change of Hydraulic Cement Mortar Exposed to a Sulfate Solution. (ASTM Philadelphia, PA).
22. Akpinar P., Casanova I. (2010) A combined study of expansive and tensile strength evolution of mortars under sulfate attack: implications on durability assessment. *Mater. Construcc.* 65(317): 59–68. https://doi.org/10.3989/mc.2010.47908
23. ASTM C-150 Standard Specification for Portland Cement (2007) (ASTM Philadelphia, PA).
24. Mendham, J., Denney, R.C., Barnes, J. D., Thomas, M. J. K. Vogel, (2000). Textbook of Quantitative Chemical Analysis (6th ed.). Pearson Education Limited. Edinburg Gate. Prentice Hall. England
25. Cimentos: determinação de teor em sulfatos. LNEC Especificações E61, Lisboa, 1979
26. Cunha, M.P.T. (2011), Desenvolvimento e avaliação de um sistema de monitorização da corrosão electroquímica no betão armado. Ph.D. Thesis. Universidade de Aveiro (in Portuguese).
27. Pavlík, V., Bajza A., Rouseková I., Uncik S., Dubík M. (2007). Degradation of concrete by flue gases from coal combustion. *Cem. Concr. Res*. 37(7): 1085–1095. https://doi.org/10.1016/j.cemconres.2007.04.008
28. Obserholster, R. E., Pore Structure, Permeability and Diffusivity of Hardened Cement Paste and Concrete in Relation to Durability: Status and Prospects, Proceedings, 8th International Congress on the Chemistry of Cement, Rio Janeiro, Brazil, Sub-Theme 4.1, September 1986, 323–335.
29. Stratful, R. F., (1964) Effect on Reinforced Concrete in Sodium Chloride and Sodium Sulfate Environments Materials Protection. 3(12), pp. 74–80.